Scientific Herald of Uzhhorod University
Series "Physics"

Journal homepage: https://physics.uz.ua/en
Issue 54, 67–79
Received: 31.07.2023. Revised: 06.11.2023. Accepted: 18.12.2023

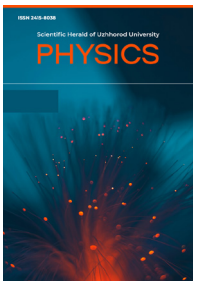

UDC 53.087
PACS 61.66
DOI: 10.54919/physics/54.2023.67

Crystal structure of barium manganese vanadate $BaMnV_2O_7$

Viktor Zavodyannyi*
PhD in Physical and Mathematical Sciences, Associate Professor
Kherson State Agrarian and Economic University
25031, 5/2 Universytetskyi Ave., Kropyvnytskyi, Ukraine
https://orcid.org/0000-0002-8224-8215

Mykola Voloshyn
PhD in Technical Sciences, Associate Professor
Kherson State Agrarian and Economic University
25031, 5/2 Universytetskyi Ave., Kropyvnytskyi, Ukraine
https://orcid.org/0000-0003-0467-1963

Valentina Zubenko
PhD in Technical Sciences, Associate Professor
Kherson State Agrarian and Economic University
25031, 5/2 Universytetskyi Ave., Kropyvnytskyi, Ukraine
https://orcid.org/0000-0002-8401-755X

Ruslan Teliuta
PhD in Technical Sciences, Associate Professor
Central Ukrainian National Technical University
25006, 8 Universytetskyi Ave., Kropyvnytskyi, Ukraine
https://orcid.org/0000-0002-4923-1227

Serhii Kvitka
PhD in Technical Sciences, Associate Professor
Dmytro Motornyi Tavria State Agrotechnological University
69600, 66 Zhukovskyi Str., Zaporizhzhia, Ukraine
https://orcid.org/0000-0001-9234-9274

Abstract

Relevance. The development of materials with excellent dielectric properties is crucial for modern telecommunications. The value of this study lies in the importance of examining these properties in the context of expanding possibilities for high-frequency applications in modern telecommunication technologies, including 4G and 5G communication.

Purpose. The purpose of this study is to investigate the crystal structure of the compound $BaMnV_2O_7$ and its dielectric properties.

Suggested Citation:
Zavodyannyi A, Voloshyn M, Zubenko V, Teliuta R, Kvitka S. Crystal structure of barium manganese vanadate $BaMnV_2O_7$. *Sci Herald Uzhhorod Univ Ser Phys.* 2023;(54):67–79. DOI: 10.54919/physics/54.2023.67

*Corresponding author

Methodology. To achieve the set purpose, methods of analysis, experimentation, comparison, and computer modelling were used. Within this study, the material of low-temperature co-fired ceramics (LTCC) was thoroughly examined, known for its high efficiency as moisture protection.

Results. A structural model for the compound $BaMnV_2O_7$ was proposed and investigated. In particular, it was found that the radius of Mn^{2+} (0.75 Å) is almost identical to the radius of Zn^{2+} (0.68 Å), confirming the similarity of the crystal structures of $BaMnV_2O_7$ and $BaZnV_2O_7$. The main results showed that pyrovanadate has a monoclinic symmetry and has a spatial symmetry group P121/c1 (14), characterised by lattice parameters: a = 5.6221(5) Å, b = 15.271(1) Å, c = 9.7109(8) Å, β = 123.702(3)°. The divergence factor was 9.05, indicating the model's correspondence to experimental data. Additionally, the density of the compound was calculated, amounting to 4.2699 g/cm^3.

Conclusions. Experimental data confirmed the presence of interatomic distances within 1.33-3.47 Å. The minimum interatomic distance in the compound structure is 1.33 Å between oxygen (O5) and vanadium (V2) atoms. The maximum interatomic distance is 3.47 Å observed between oxygen (O1) and (O2) atoms. With characteristics such as low dielectric permittivity (εr~8.9) and a high quality factor coefficient (Qu×f 31362 GHz), the compound $BaMnV_2O_7$ exhibits excellent microwave dielectric properties. The practical value of the obtained results lies in the potential development and improvement of materials with high dielectric properties, such as $BaMnV_2O_7$, for their application in telecommunication technologies, contributing to the development of more compact and reliable components for electronics

Keywords: X-ray structural analysis; dielectric properties; Bragg-Brentano geometry; Rietveld method; resonator

Introduction

Since 2013, there has been a rapid development of cellular communication, which requires materials with exceptional dielectric characteristics. Properties such as high quality factor, low temperature coefficient of resonant frequency, and excellent relative dielectric permittivity are critical for the further development of this area. In this context, low-temperature co-fired ceramics (LTCC) emerge as one of the promising materials. The ability to sinter at temperatures below 1000°C and the use of more readily available materials, such as copper, make LTCC technology particularly attractive. In addition, ceramics offer cost-effectiveness and ease of manufacturing devices, moisture tightness, and reliability even under significant temperature fluctuations. For instance, in radar systems, active phased array antennas consisting of receiver-transmitter modules are employed for optimisation and size reduction. L.O. Roman [1] notes that the miniaturisation of such devices led to the adoption of LTCC multilayer board technology.

It is essential to highlight that this technology also allows for the creation of complex multilayer boards. O.A. Nemyrovych [2] mentions that during LTCC technology, metallisation occurs through screen printing on an unfired ceramic sheet. The sheets are assembled into a stack, rolled on rollers, and sintered at temperatures up to 950°C, allowing the use of materials like silver or copper. The thickness of the resulting conductors is approximately 10 micrometres, roughly corresponding to three skin depths at 1 GHz. LTCC technology is particularly suitable for manufacturing planar high-Q inductors, resonators, and planar resistors. In the work of D.I. Varvaruk [3], the PBA 313 01/2 is investigated, representing an edge cascade for a Bluetooth communication system. It utilises ball grid array (BGA) connectors, and all individual components are located on one side of the board. This board is manufactured using LTCC technology and consists of 6 layers of this ceramic and 7 metal layers, confirming the possibility of creating multilayer boards. Moreover, Ye.M. Yashchyshyn [4] indicates that the advantages of LTCC include the ability for three-dimensional system integration, high control of technological parameters to ensure high repeatability, flexibility regarding the number of layers and types of materials, achieving minimal line and gap widths (on the order of 50 microns), the possibility of integrating passive and distributed elements, and mounting integrated circuits.

Many materials are considered for potential use in LTCC. However, vanadates attract special attention because they exhibit important properties that can be useful for high-frequency applications. For example, T.M. Hrychanovska & I.Yu. Protsenko [5] note that VO_2 films undergo a phase transition with increasing temperature, accompanied by a significant decrease in specific resistance. This property allows their use as thermoresistors for effective thermal protection at high temperatures. According to S.V. Khalameida *et al.* [6], the use of a V_2O_5 wet gel and hydrothermal treatment allowed obtaining magnesium pyro- and orthovanadates. Samples obtained

by microwave-assisted hydrothermal treatment are characterised by a high specific surface area and a developed porous structure.

Pyrovanadates are known for their complex crystalline structure, including atoms of chemical elements arranged in a specific lattice. These characteristics of the crystalline structure influence its physical and electronic properties and determine the magnetic and dielectric characteristics of the compound. However, information about the crystalline structure of $BaMnV_2O_7$ is not yet fully revealed, and the parameters of the lattice microstructure remain unknown. Therefore, the analysis of LTCC ceramic properties, including its crystalline structure, is especially relevant and crucial for developing modern telecommunications technologies. The purpose of this study is to analyse the crystalline structure and dielectric characteristics of the $BaMnV_2O_7$ compound. The high dielectric permittivity under certain conditions and frequencies makes the compound an interesting material for use in telecommunications technologies, where having materials with high dielectric properties for manufacturing resonators, filters, and other components is crucial.

Materials and Methods

To achieve the purpose of this study, various methods were employed, including analysis, comparison, experimental investigations, and computer modelling. All measurements and analyses were conducted under specialised laboratory conditions, where necessary temperature and humidity parameters were ensured. The obtained results underwent further scrutiny, and their reliability was subjected to additional verification and analysis.

The analysis method allowed for a detailed examination and breakdown of experimental and computational data to reveal the peculiarities of the crystalline structure of the $BaMnV_2O_7$ compound. During the comparative analysis, properties of $BaMnV_2O_7$ were juxtaposed with other materials exhibiting high dielectric characteristics, providing insights into its potential applications. For the experiments, $BaMnV_2O_7$ samples were prepared according to detailed protocols, involving synthesis and purification to obtain pure material for further investigations. Experimental measurements of dielectric properties and other physical parameters of the $BaMnV_2O_7$ compound provided specific data for analysis and justification of material properties. For the analysis, the diffraction spectrum of the compound was utilised using the PDF-2 No. 044-0245 database, containing theoretical and experimental data of powder diffractograms collected under conditions of radiation on a copper filter with Bregg-Brentano geometry [7]. The spectrum was analysed using the HighScore Plus 3.0 programme (Netherlands) to ensure its correspondence to a single-phase state of the $BaMnV_2O_7$ compound. Indexing of the diffraction spectrum was performed to determine the crystalline structure of the $BaMnV_2O_7$ compound. The built-in TREOR module in this programme was used to index the diffraction spectrum. Furthermore, using the structural model for the β-$BaZnV_2O_7$ phase, refinement of microstructural parameters was conducted using the Rietveld method and the HighScore Plus 3.0 programme. Key characteristics of the crystal structure of pyrovanadate were obtained.

Using computer modelling allowed for a detailed analysis of the crystalline structure and properties of $BaMnV_2O_7$ using modern computational technologies. The combination of these diverse methods provided a comprehensive understanding of the $BaMnV_2O_7$ compound, including its crystalline structure and physical characteristics. Specific protocols for result analysis were developed for each of the methods used. This included processing diffraction patterns, phase identification, determination of crystalline structure parameters, and more. To confirm the reliability and accuracy of the obtained results, series of repeated experiments were conducted, and the obtained data were compared with literature sources. Considering the large amount of data, a statistical analysis was performed to confirm the results and determine the degree of their deviation.

The study paid special attention to the analysis of the crystalline structure and physical properties of the $BaMnV_2O_7$ compound. The combination of methods, including X-ray structural analysis, computer modelling, and other spectroscopic and physical methods, provided an opportunity to gain a comprehensive understanding of the crystalline structure and physical properties of the $BaMnV_2O_7$ compound.

Results

It follows from the literature that vanadates have satisfactory microwave dielectric properties and can be used as microwave LTCC ceramics [8]. Microwave dielectric ceramics are an important class of materials for the production of electronic devices, especially high-frequency and microwave devices. It is characterised by high permittivity and low losses, which allow effectively using these materials for transmitting signals in the high-frequency range. In addition, it is important to note that vanadates can be integrated into LTCC technology. This means that they can be used as components of the material used for the manufacture of microwave devices by co-heating at low temperatures.

$BaMnV_2O_7$ is also a promising material for use in LTCC technology. Given that the radius Mn^{2+} (r = 0.75 Å) is close to Zn^{2+} (r = 0.68 Å), a crystal structure similar to the $BaZnV_2O_7$ compound should be expected [6]. This similarity in crystal structures is due to the close values of the sizes of Mn^{2+} and Zn^{2+} atoms, which leads to similar ways of ordering

them in the crystal lattice of both compounds. This pyrovanadate has two polymorphic modifications, i.e. it can exist in two different crystal structures under the same temperature and pressure conditions. Crystal structure of low-temperature β-$BaZnV_2O_7$ crystallises in monoclinic syngony, spatial symmetry group (PGS) $P2_1/n$, grid parameters a = 5.573 A^0, b = 15.175 A^0, c = 7.429 A^0, β = 96.45^0. The data show that there is a certain degree of irregularity in the crystal lattice, but simultaneously, there is a plane of symmetry. The microstructural parameters are shown in Table 1 and indicate small-scale features of the material's crystal structure. Small-scale features indicate details and relationships between atoms or other components in the crystal structure of a material.

Table 1. Microstructural parameters of β-$BaZnV_2O_7$

Atom	Wyck	X/a	y/b	z/c
Ba	4e	-0.2830(1)	0.28596(3)	0.4471(7)
Zn	4e	-0.2077(2)	0.05006(6)	0.3676(1)
V1	4e	-0.2525(2)	0.36597(8)	0.6654(2)
V2	4e	-0.2052(2)	0.56203(8)	0.7105(2)
O1	4e	-0.246(1)	0.2824(4)	0.5224(8)
O2	4e	-0.256(1)	0.4716(4)	0.5530(8)
O3	4e	-0.229(1)	0.6604(4)	0.617(1)
O4	4e	0.077(1)	0.5527(4)	0.8214(9)
O5	4e	-0.414(1)	0.5542(4)	0.8681(8)
O6	4e	-0.494(1)	0.3553(4)	0.7904(9)
O7	4e	0.005(1)	0.3609(4)	0.8099(9)

Source: compiled by the authors

The structure of β-BaZnV was taken as the initial model of the crystal structure$_2O_7$. Selection of the initial model of the β-$BaZnV_2O_7$ crystal structure in the examination of $BaMnV_2O_7$ is based on several reasons. First, both compounds have the same composition and arrangement of atoms, which may indicate the similarity of their crystal structures. Secondly, the ability to use an already examined model simplifies the analysis and comparison of the properties of a new compound. Furthermore, if β-$BaZnV_2O_7$ was the subject of previous research, the availability of known data facilitates the analysis of $BaMnV_2O_7$. In addition, the affinity of the components Ba, Mn, V, Zn, and O emphasised the similarity of the structures of these compounds.

As a result of the conducted analysis of the structural characteristics of the $BaMnV_2O_7$ compound, it was established to crystallise in monoclinic syngony and have a P121/c1 spatial symmetry group [14]. Monoclinic syngony indicates that the crystal structure of the compound has irregularity, which manifests itself in the form of uneven sides and angles in a parallelogram that restricts the base region. In this case, the main axes of the crystal are not mutually perpendicular, and therefore, the connection exhibits symmetry with respect to only one plane. In the $BaMnV_2O_7$ crystal lattice, the plane of symmetry inequalities is present, as in β-$BaZnV_2O_7$. The specific lattice parameters are: a=5.6221(5)A0, b = 15.271(1)A0, c = 9.7109(8) A0 at β = 123.702(3)0. The specified lattice parameters (a, b, c, and β) determine the geometric dimensions and angles between the lattice vectors. The values a, b, and c represent the lengths of the axes, and β determines the angle between a and c. Table 2 shows the microstructural parameters for detailed analysis.

Table 2. $BaMnV_2O_7$ microstructural parameters

Atom	Wyck	s.o.f.	x	y	z
Ba1	4e	1	0.403(2)	0.2068(4)	0.6468(8)
V1	4e	1	0.930(3)	0.1236(9)	0.130(2)
V2	4e	1	0.954(4)	0.948(1)	0.240(2)
Mn1	4e	1	0.595(4)	0.442(1)	0.874(2)
O1	4e	1	0.81(1)	0.220(3)	0.079(4)
O2	4e	1	0.84(1)	0.823(4)	0.724(7)
O3	4e	1	0.92(1)	0.855(3)	0.107(5)
O4	4e	1	0.73(1)	0.960(3)	0.276(5)
O5	4e	1	0.825(8)	0.523(3)	0.570(5)
O6	4e	1	-0.107(9)	0.190(3)	0.311(4)
O7	4e	1	0.825(9)	0.103(3)	0.340(3)

Source: compiled by the authors

Important experimental data for the characterisation of crystalline materials are the values of interplanetary distances. Interplanetary distances indicate the distances between atoms and molecules located on different planes of the crystal lattice [9]. The intensity, i.e. the strength of the diffraction signal that is recorded during the crystal examination, also depends on the structural features of the crystal, such as the position of atoms and their interplanetary distances. The divergence factor (R-factor) is 9.05, and the calculated density is 4.2699 g/cm^3. If the interplanetary distances differ by 0.03A_0, the diffraction lines are taken as one. The values of interplanar distances and intensities calculated using this model are shown in Table 3. This position was considered when analysing the crystal structure, and according to these data, the $BaMnV_2O_7$ structure is represented.

Table 3. Values of interplanar distances and intensities calculated for the structure of the $BaMnV_2O_7$ compound

$2\theta_{cal}$	$2\theta_{obs}$	d_{cal}	d_{obs}	I_{cal}	I_{obs}	H	K	L
11.5723	11.574(5)	7.64064	7.63951	4.46	3.16	0	2	0
13.3377	13.344(4)	6.63302	6.62968	2.87	4.17	0	1	-1
16.7107	-	**5.301**	-	0.21	-	0	2	-1
16.7107	-	**5.301**	-	0.21	-	0	2	1
16.853	-	**5.25656**	-	0.08	-	1	1	-1
18.9506	18.957(5)	4.67918	4.67769	1.12	3.18	1	0	0
19.6453	19.650(6)	4.51526	4.51408	5.99	3.06	1	2	-1
19.8285	19.839(6)	4.47395	4.47163	2.17	3.03	1	1	0
20.8258	-	**4.2619**	-	0.8	-	1	0	-2
21.1981	21.19(1)	4.18788	4.18901	1.24	1.06	0	3	-1
21.6308	21.619(4)	4.10508	4.10738	5.05	4.23	1	1	-2
22.2635	22.263(2)	3.98983	3.98994	15.34	13.12	1	2	0
23.2727	23.266(5)	3.81905	3.82015	0.21	3.05	0	4	0
23.6007	23.610(8)	3.7667	3.76525	2.1	1.83	1	3	-1
23.891	23.892(2)	3.72159	3.72138	16.5	15.85	1	2	-2
24.1616	24.1646(6)	3.68052	3.68007	64.23	66.81	0	0	2
24.8641	24.8607(5)	3.5781	3.57858	45.96	88.96	0	1	-2
25.8398	25.845(4)	3.44516	3.44451	6.34	4.14	1	3	0
26.269	-	**3.38984**	-	1.86	-	0	4	-1
26.269	-	**3.38984**	-	1.86	-	0	4	1
26.8685	-	**3.31555**	-	0.26	-	0	2	-2
26.8685	-	**3.31555**	-	0.26	-	0	2	2
27.267	27.264(1)	3.26799	3.26834	23.26	17.78	1	3	-2
28.2674	28.277(1)	3.15457	3.1535	100	99.98	1	4	-1
28.2908	28.279(1)	3.15201	3.15325	89.19	100	1	1	1
29.933	29.9314(8)	2.98271	2.98287	22.35	38.38	0	3	-2
30.1852	30.184(1)	2.95837	2.95847	15.33	19.83	1	4	0
30.8755	30.8743(9)	2.89378	2.89389	33.11	30.7	1	1	-3
31.4309	-	**2.8439**	-	3.42	-	1	4	-2
31.9536	31.9486(9)	2.79856	2.79899	29.52	28.9	2	0	-2
32.8753	32.892(2)	2.72218	2.72086	9.27	8.24	1	3	1
33.7987	33.782(4)	2.64988	2.65113	0.65	4.22	0	4	-2
35.1563	35.2(1)	2.5506	2.55051	16.78	9.58	1	3	-3
35.1795	35.18(7)	2.54898	2.54864	0.36	9.47	2	2	-1
35.8705	-	**2.50144**	-	0.06	-	2	1	-3
36.463	36.478(3)	2.46214	2.46118	5.07	6.2	1	4	1
37.0835	37.111(2)	2.42236	2.4206	3.33	11.92	0	1	-3
37.347	37.357(1)	2.40587	2.40527	10.02	22.98	0	6	-1
38.5105	38.5(1)	2.33582	2.33571	0.36	5.52	0	2	-3
38.5587	38.55(4)	2.33301	2.33359	11.01	5.51	1	4	-3
38.5875	38.60(4)	2.33133	2.33041	0.75	3.53	1	0	2
38.8313	38.82(1)	2.31725	2.31781	0.52	2.54	1	6	-1

Table 3. Continued

$2\theta_{cal}$	$2\theta_{obs}$	d_{cal}	d_{obs}	I_{cal}	I_{obs}	H	K	L
38.9206	38.950(5)	2.31214	2.31049	2.74	9.56	2	1	0
39.0525	39.071(4)	2.30464	2.3036	12.96	11.68	1	1	2
39.9081	39.927(7)	2.25718	2.25616	0.01	2.12	2	4	-2
40.861	40.821(2)	2.20671	2.2088	2.32	8.28	2	4	-1
41.561	41.538(5)	2.17115	2.17232	2.28	3.22	1	0	-4
41.9985	41.991(3)	2.14954	2.14989	2.88	6.16	1	1	-4
42.593	42.587(1)	2.1209	2.1212	2.98	15.92	1	5	-3
42.8215	42.815(3)	2.11011	2.11041	9.66	8.79	2	1	-4
43.2112	43.2(1)	2.09198	2.09297	2.74	6.23	0	7	1
43.2895	43.2(1)	2.08838	2.0918	0.7	6.22	1	2	-4
43.8265	43.81(6)	2.06403	2.0648	5.92	11.25	0	4	-3
43.8394	43.84(5)	2.06345	2.0633	0.4	10.4	2	5	-2
45.3733	45.4(1)	1.99719	1.99787	0.43	9.68	1	6	1
45.3754	45.38(6)	1.9971	1.99672	14.34	9.38	1	3	-4
46.1501	46.156(3)	1.96536	1.96513	0.04	5.21	2	3	-4
46.5094	46.509(4)	1.95102	1.95103	0.9	4.18	2	5	-3
47.4955	47.501(6)	1.91279	1.91259	5.44	9.45	0	5	-3
47.5903	47.54(2)	1.9092	1.91124	2.55	4	0	8	0
49.1616	49.159(8)	1.85179	1.85188	0.01	6.18	3	1	-3
49.2685	49.25(2)	1.84802	1.84853	0.42	3.01	0	8	-1
49.4989	49.501(1)	1.83995	1.83990	16.11	28.86	0	0	4
50.4662	50(1)	1.80693	1.807	2.23	7.04	1	8	-1
50.4805	50(1)	1.80645	1.80699	3.1	7.04	1	7	1
51.0418	51.04(9)	1.7879	1.78791	3.47	5.42	1	1	3
51.6071	51.07(9)	1.76963	1.78686	0.19	5.42	1	5	-4
51.6547	51.6(1)	1.76812	1.76867	0.11	1.24	3	0	-4
51.6701	51.7(3)	1.76763	1.76745	1.48	1.13	1	8	0
52.1158	52.102(5)	1.75355	1.75397	1.29	3.2	1	7	-3
52.8668	52.846(5)	1.7304	1.73103	0.73	3.15	0	3	-4
53.1268	53.139(4)	1.72254	1.72217	0.09	4.13	3	2	-4
53.1345	54.717(4)	1.72231	1.67619	0.25	4.06	2	6	0
54.928	54.928(3)	1.67024	1.67023	1.3	6.05	3	3	-4
55.3854	55.343(7)	1.65752	1.65868	0.12	5.94	0	4	-4
55.3854	55.5(1)	1.65752	1.65442	0.12	3.41	0	4	4
55.5197	55.54(7)	1.65383	1.65333	2.84	3.41	2	7	-3
56.1183	56.129(4)	1.6376	1.63732	3.03	4.03	2	5	1
56.3901	56.388(2)	1.63035	1.6304	1.78	8.09	0	7	-3
57.0776	57.10(4)	1.61233	1.61182	0.01	1.25	1	3	-5
57.1508	57.18(1)	1.61044	1.60961	4.32	2.88	2	0	2
57.5574	57.520(5)	1.60003	1.60099	2.02	4.95	2	4	-5
57.7379	57.71(9)	1.59546	1.59616	0.5	3.46	2	7	0
57.7448	57.75(4)	1.59528	1.59524	0.07	3.16	1	9	0
58.4963	58.507(5)	1.57657	1.5763	0.28	3.15	1	9	-2

Source: compiled by the authors

However, not all lines meet this criterion. Lines that do not meet this criterion are shown in bold in Table 3. As can be seen from the calculation table, such diffraction lines have a low intensity and, therefore, may not be detected in the diffraction spectrum. All observed strong lines coincide with the lines calculated using this structural model. In addition, the discrepancy factor is less than 10% and is 9.05%. The R-factor is one of the criteria used to evaluate the suitability of a structural model for experimental data [10]. It indicates a correspondence between the measured data and those obtained using the model.

A low R-factor (less than 10%) indicates that the structural model correctly describes the experimental data, so it can be assumed that the proposed structural model of the crystal structure of a given compound is correct. Ultimately, Zn and Mn are similar in their properties and can have a similar structure for the $BaZnV_2O_7$ compound. Table 4 shows the interatomic distances for the $BaMnV_2O_7$ structural model.

Table 4. Interatomic distances of the $BaMnV_2O_7$ compound structural model

Ba1		V1		V2		Mn1	
- O6	2.77(3)	- O2	1.47(6)	- O5	1.33(4)	- O7	1.63(6)
- O6	2.78(5)	- O1	1.58(4)	- O4	1.47(7)	- O4	2.07(6)
- O2	2.80(6)	- O6	2.00(5)	- O3	1.79(5)	- O2	2.77(8)
- O2	2.83(8)	- O7	2.26(5)	- O7	2.76(5)	- O6	2.87(6)
- O4	2.84(5)	- O5	2.30(4)	- V1	2.83(2)	- V2	2.91(2)
- O1	2.88(6)	- O3	2.68(6)	- Mn1	2.91(2)	- V1	3.27(2)
- O3	2.99(4)	- V2	2.83(2)	- O7	3.29(4)	- V2	3.31(3)
- O1	3.19(3)	- O5	3.18(5)	- Mn1	3.31(3)	- O5	3.31(3)
- O1	3.25(6)	- Mn1	3.27(2)			- O4	3.32(4)
- O7	3.27(4)	- O4	3.28(6)			- Mn1	3.45(3)
- O3	3.30(5)						
O1		**O2**		**O3**		**O4**	
- V1	1.58(4)	- V1	1.47(6)	- V2	1.79(5)	- V2	1.47(7)
- O6	1.88(6)	- O6	1.7(1)	- O5	1.92(6)	- Mn1	2.07(6)
- O2	1.89(6)	- O1	1.89(6)	- O6	2.67(6)	- O5	2.18(8)
- Ba1	2.88(6)	- O7	2.5(1)	- V1	2.68(6)	- O7	2.24(7)
- O7	2.88(6)	- Mn1	2.77(8)	- O4	2.79(8)	- O3	2.79(8)
- O6	3.00(7)	- Ba1	2.80(6)	- Ba1	2.99(4)	- Ba1	2.84(5)
- O3	3.02(8)	- Ba1	2.83(8)	- O1	3.02(8)	- O7	3.04(4)
- O3	3.10(5)	- O3	3.03(9)	- O2	3.03(9)	- O5	3.07(5)
- Ba1	3.19(3)	- O3	3.19(9)	- O1	3.10(5)	- V1	3.28(6)
- Ba1	3.25(6)	- O1	3.47(7)	- O2	3.19(9)	- Mn1	3.32(4)
- O7	3.47(6)			- Ba1	3.30(5)		
- O2	3.47(7)						
O5		**O6**		**O7**			
- V2	1.33(4)	- O7	1.45(7)	- O6	1.45(7)		
- O3	1.92(6)	- O2	1.7(1)	- Mn1	1.63(6)		
- O4	2.18(8)	- O1	1.88(6)	- O4	2.24(7)		
- V1	2.30(4)	- V1	2.00(5)	- V1	2.26(5)		
- O5	2.93(7)	- O3	2.67(6)	- O2	2.5(1)		
- O7	3.06(6)	- Ba1	2.77(3)	- V2	2.76(5)		
- O4	3.07(5)	- Ba1	2.78(5)	- O1	2.88(6)		
- V1	3.18(5)	- Mn1	2.87(6)	- O4	3.04(4)		
- O5	3.22(6)	- O1	3.00(7)	- O5	3.06(6)		
- Mn1	3.31(3)			- Ba1	3.27(4)		
				- V2	3.29(4)		
				- O1	3.47(6)		

Source: compiled by the authors

Minimum interatomic distance is 1.33A^0 O5-V2. Maximum interatomic distance is 3.47A^0 O1-O2. Interatomic distances are key crystal structure parameters and determine atoms' relative position in the crystal lattice. In crystal lattices, the atoms are arranged in an ordered manner, forming various structural elements, such as cubes, tetrahedra, and octahedra [11]. The distances between these structural elements determine interatomic distances. For example, interatomic distances indicate the distances between atoms for metal crystal lattices. In the context of the $BaMnV_2O_7$, interatomic distances indicate the distances between barium (Ba), manganese (Mn), vanadium (V), and oxygen (O) atoms in the crystal lattice. The interatomic distances between these atoms affect the electronic structure and, consequently, the conductivity of the compound. These distances are important for understanding the properties of a material, such as

magnetic, electronic, and dielectric, because of their effect on electron motion. In addition, interatomic distances indicate possible interactions between atoms in a compound that affect its properties and behaviour under various conditions.

In metals, electrons in the outer shell of atoms, known as "free electrons", can separate from atoms and move freely along the crystal lattice. If the interatomic distances in the metal crystal decrease, the electrons will have less space to move. This can increase the effective concentration of free charge carriers since the electrons will interact more with each other. As a result, the conductivity of the material may increase. In contrast, if the interatomic distances increase, the electrons will have more space to move. This can lead to a decrease in the effective concentration of free charge carriers and, accordingly, to a decrease in conductivity. According to this, if the interatomic distances in $BaMnV_2O_7$, the electrons in the manganese and vanadium sublattices decrease, they will have less space to move. This can lead to an increase in the effective concentration of free charge carriers, which will make the material a better conductor. In contrast, if the interatomic distances increase, the electrons will have more space to move. This can lead to a decrease in the effective concentration of free charge carriers and, accordingly, to a decrease in conductivity [12].

In the crystal structure of the $BaMnV_2O_7$ compound, two Ba+2 arrangements are observed, each of which has special bonds with oxygen and vanadium atoms and different configurations of Mn atoms. In Figure 1, Ba+2 is bound to four oxygen atoms O1, O2, O4, O6, and in another modification, the atom has a different arrangement of O1, O2, O2, and O3. O4, O6. The Vanadium atom also has two locations. V1 forms triangular bonds with oxygen atoms O1, O6. Another arrangement of V2 forms an irregular tetrahedron with oxygen atoms O3, O4, and O5. Two Mn atoms form triangular bonds with oxygen atoms O4, O7, the other arrangement of the manganese atom has a bond with the oxygen atom O7.

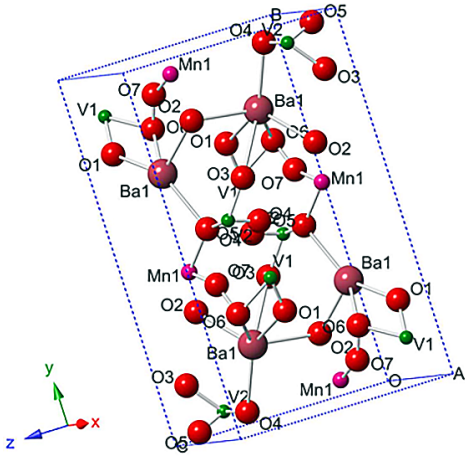

Figure 1. Image of the crystal structure of the $BaMnV_2O_7$ compound
Source: compiled by the authors

In further analysis of the crystal structure of the $BaMnV_2O_7$, this structure affects the electronic and electrical properties of the material. For example, the arrangement of Ba^{+2} atoms and their bonds with oxygen and vanadium atoms can determine the efficiency of charge transfer in a material. It is also important to consider that different configurations of Mn atoms can affect the magnetic properties of the compound. The arrangement of Ba^{+2} atoms and their bonds with oxygen and vanadium atoms can affect the efficiency of charge transfer in a material through two main mechanisms: changes in the valence or degree of ionisation of atoms and changes in the electronic structure. In the specific case of a $BaMnV_2O_7$ compound, the arrangement of Ba^{+2} atoms affects the location and structure of charge carriers in the material. This leads to a change in its electrical conductivity.

As for Mn atoms, their different configurations can affect the magnetic properties of the compound. The orientation and spin structures of the atoms determine the magnetic properties of a material. Changes in the crystal structure and arrangement of Mn atoms lead to changes in magnetic properties, such as magnetic susceptibility, magnetic separation coefficient, and spin resonance frequency. These aspects of magnetic properties may be the subject of additional experiments to understand better the physical mechanisms that determine the magnetic behaviour of the $BaMnV_2O_7$ compound. The application of $BaMnV_2O_7$ in LTCC ceramics can open up new opportunities for the production of high-frequency devices with excellent stability and efficiency. $BaMnV_2O_7$ shows substantial potential for application in LTCC due to its satisfactory microwave dielectric properties. The main characteristics of

the compound, such as its low permittivity (er ~ 8.9), high quality factor (Qu×f 31362 GHz) and excellent thermal stability, make it an attractive candidate for use in the manufacture of microwave devices.

However, on the dielectric characteristics of $BaMnV_2O_7$, various factors can influence understanding, which is important for optimising the characteristics of the material. For example, changes in the crystal structure. Since the permittivity of a material depends on the internal lattice and the location of atoms, any changes in the crystal structure can affect the dielectric properties. The presence of impurities or irregularities in the crystal structure can affect the conductivity and dielectric properties. If defects in the crystal structure (for example, gaps in the lattice, inconsistencies in the atomic arrangement) or impurities are present, the conductivity and dielectric properties are changed. Defects can be charged, which also affects electrical behaviour. In addition, microscopic features such as grain boundaries and inclusions also change electrical behaviour. Dielectric properties often change with temperature changes. Thermal exposure can lead to changes in the crystal structure and dielectric parameters. As the temperature rises, the atoms move and change their position in the lattice, affecting the electrical properties. Material processing also plays an important role in the manufacture of devices [13].

In many cases, LTCC ceramics are used to make RF electronics components, and $BaMnV_2O_7$ can be an important material for optimising such devices. This material can be particularly valuable for developing new telecommunications and microwave technologies components, where low losses and high frequency stability are critical factors. The results obtained create prospects for further research and possible implementation of $BaMnV_2O_7$ in the telecommunications technology industry, including modern 5G networks.

Discussion

LTCC ceramic is an important material in modern technologies for the production of microwave appliances. It allows manufacturing devices with high dielectric properties and low signal loss at high frequencies. However, the use of LTCC ceramics has some drawbacks. One of the main disadvantages is the physico-chemical incompatibility of many thick-film materials with LTCC sheets, which makes them difficult to use simultaneously. In the study by H. Birol et al. [14], it is indicated that chemical problems occur due to the interaction of the glass phase in the tape and thick films, while physical problems are usually associated with the discrepancy between the shrinkage of the tape and the paste for screen printing. This is observed microscopically and macroscopically in chemical diffusion (using microscopy and spectroscopic analysis) or deformed structures (warping, stratification, twisting), respectively. In addition, deformations such as warping, conductor inflating, and peeling can occur during the ceramic sintering process. This clearly affects the quality of devices manufactured using this technology. In addition, the compatibility of LTCC materials with other components of electronic devices can cause certain difficulties. Since they can have different thermal expansion coefficients, this can cause mechanical stresses and affect the reliability of the device in general.

Despite some of the shortcomings of LTCC ceramics, intensive research is being conducted to optimise it and find new compounds that can be applied in electronics and telecommunications technologies. Among the representatives of LTCC ceramics, a number of vanadates can be distinguished, the dielectric properties and crystal structure of which are intensively examined. One of the most interesting alternatives is pyrovanadate ceramics, which has already attracted the attention of researchers for its unique properties and potential applications in modern technologies. In the study of Y.T. Huang *et al.* [16], it was reported that the results of a study of the dielectric properties and crystal structure of $SrCo1\text{-}xMgxV_2O_7$ (x = 0-0.09) LTCC ceramics. It is indicated that the $SrCoV_2O_7$ compound crystallises in monoclinic syngony with the spatial symmetry group P21/c (14). Due to its dielectric properties, this compound is promising as a microwave dielectric ceramic. Microwave dielectric ceramics have specific dielectric properties at high frequencies, especially in the microwave range. $NaCa_4V_5O_{17}$ ceramics manufactured using LTCC technology (at temperatures of 780-860°C), attracts attention as a potential candidate for use in the production of microwave devices. The results, provided in study by C. Yin *et al.* [17], demonstrate that the compound crystallises in triclinic syngony, and has promising dielectric properties (permittivity εr = 9.72, Q-factor Q×f = 51000 GHz, and temperature coefficient of resonant frequency τf = -84 · 10-6 1/°C) and can be used in multilayer electronic devices.

Authors A.N. Unnimaya *et al.* [18] reported the results of the examination of $Mg_4V_2O_9$ ceramics, which show high efficiency in the microwave range and also demonstrate good chemical compatibility. It is indicated that by its properties, the compound can be used for the fairing designs of terahertz (THz) antenna arrays. According to experiments of D. Zhou *et al.* [19], microwave dielectric ceramics $(1\text{-}x)BiVO_4\text{-}xTiO_2$ (x = 0.4, 0.5, 0.55, and 0.60) in low-temperature firing was obtained by the conventional solid-phase reaction method. According to the results of the study, ceramics can be used as a substrate for physically and electrically small dielectric microstrip antennas. In the study by E.K. Suresh *et al.* [20], the dielectric properties of a16v18o61 ceramics (a = Ba, Sr, Ca) were measured using a vector network analyser, which showed

high-quality coefficients in the absence of load. Together with 0.4 $BaTa_2V_2O_{11}$-0.6 $Ba_2BiV_3O_{11}$ composite material, potential high-frequency compounds.

Given the importance of microwave ceramics in modern technologies, especially in the context of 4G cellular communication and its further development in 5G, it is important to consider its properties and potential for optimising and improving high-frequency signal transmission. Results of the examinations of the $BaMnV_2O_7$ LTCC indicate the high potential of this material as a microwave dielectric ceramic, in particular, due to its low sintering temperature and impressive microwave dielectric characteristics, indicating possible use in modern and future communication systems. Notably, the examined compound $BaMnV_2O_7$ fits in with the general trend of pyrovanadates in terms of crystal features. Regularities in the crystal features and dielectric properties of $BaMnV_2O_7$, consist in their similarity in terms of interatomic distances and the base crystal structure. This indicates a certain conservatism of the pyrovanadate group in these aspects. However, it should be considered that individual differences may occur due to the influence of valence and the location of atoms in the structure. In comparison with the results of studies of other compounds, it can be noted that $BaMnV_2O_7$ has close interatomic distances characteristic of pyrovanadates. The atoms' arrangement and coordination are also similar to other vanadates examined. Additional research, in particular, dielectric studies, allows a better understanding of the properties of these compounds and their potential applications.

Common dielectric properties include parameters that characterise the ability of a material to conduct or block the flow of electric charge when exposed to an electric field. These include characteristics such as permittivity, Q-factor, loss of dielectric properties. The overall dielectric properties of a material are determined by its chemical composition, crystal structure, microstructure, and other factors. In the case of pyrovanadates like $BaMnV_2O_7$ their dielectric properties may affect their suitability for specific applications, particularly in telecommunications technologies. A study by X. Jiang *et al*. [21] showed that microwave dielectric $BaMnV_2O_7$ LTCC ceramics have high performance. For example, its permittivity (εr) is about 8.9, and the quality factor (Qu×f) is 31362 GHz. The temperature resistance is also -54.9 ppm/°C at a sintering temperature of 950°C [22]. These properties make $BaMnV_2O_7$ LTCC a promising material for use in 5G polarisation converters [23]. Compared to other materials, $BaMnV_2O_7$ LTCC is identified to be competitive. For example, $CA_3MgSi_2O_8$ ceramics have an εr of about 5.3, Qu×f reaches 60000 GHz, and τf is -15 ppm/°C, as reported by H. Barsegar-Bafrooei *et al.* [24]. In addition, the dielectric properties of ceramics Bi1.5 Mg0.8 Cu0.2 V1.5 O7 and Bi1.5 Mg0.2 Cu0.8 V1.5 O7 were examined, characterised by low permeability and higher losses according to M. Shivalingayya & R.L. Raibagkar [25].

Summarising, $BaMnV_2O_7$ LTCC exhibits excellent microwave dielectric characteristics that can be compared to or even surpass other materials used in 5G technologies [26; 27]. In particular, the high-temperature modification of $BaMnV_2O_7$ may have the potential to solve problems related to high-frequency bands in telecommunications systems [28]. Further research is needed to better understand the possibilities and potential applications of the materials under study. In particular, it is important to investigate the possibility of optimising the manufacturing processes and properties of $BaMnV_2O_7$ LTCC ceramics. This will expand the scope of its application and improve efficiency in telecommunications technologies. It is also important to consider that a detailed study of the crystal structure and properties of materials is a key stage for their successful implementation in microwave devices and 5G equipment.

Conclusions

The diffraction spectrum of the $BaMnV_2O_7$ compound was used in this study from the 2009 PDF-2 database No. 044-0245. The spectrum was captured using copper-filtered radiation with the Breg-Brentano shooting geometry and was single-phase. The HighScore Plus 3.0 programme (Netherlands) was used to analyse the crystal structure. The structural model proposed for $BaMnV_2O_7$ compound corresponds to the β-$BaZnV_2O_7$ type. This compound belongs to a monoclinic syngony with a spatial symmetry group P121/c1 (14). Using this model, specific values of the lattice constants were determined: a = 5.6221(5) Å, b = 15.271(1) Å, c = 9.7109(8) Å, and angle β = 123.702(3). The microstructural parameters that have been determined provide additional information about the orientation of crystal grains in the compound. The general trend of vanadates indicates that the $BaMnV_2O_7$ compound exhibits good dielectric properties that can make it attractive for use in telecommunications technologies, in particular, in microwave devices.

The analysis performed allows understanding how the crystal structure affects the dielectric properties of the compound, which is important for its further improvement and optimisation. In the course of the study, LTCC ceramics were considered. Although the material has its advantages, such as cost-effective device manufacturing, tightness and mechanical strength, disadvantages, such as physicochemical incompatibility with other materials and the possibility of deformation during sintering, have been identified. The detected characteristics of $BaMnV_2O_7$ open up opportunities for its use in high-frequency applications, this is an important element of modern

communication technologies. This opens up broad prospects for further research in this area. Opportunities to use the results also include the development of more compact and reliable components for electronics and the introduction of $BaMnV_2O_7$ in high-frequency applications where good dielectric characteristics of the material are important. Further research may be of great importance for developing and improving materials in the telecommunications and electronics industries.

Acknowledgements
None.

Conflict of Interest
None.

References
[1] Roman LO. X-band transceiver module. In: Materials of the II All-Ukrainian Scientific and Technical Conference of Students and Postgraduates "Radio Electronics in the XXI Century". Kyiv: National Technical University of Ukraine "Igor Sikorsky Kyiv Polytechnic Institute"; 2019:80–1.
[2] Nemyrovych OA. Temperature and frequency properties of piezoelectric crystals germano- and silicosillenites. Kyiv: National Technical University of Ukraine "Igor Sikorsky Kyiv Polytechnic Institute"; 2019. 91 p.
[3] Varvaruk DI. Development of a graphical interface and BlueTooth connection module multimedia touch keyboard. Ivano-Frankivsk: King Danylo University; 2021. 111 p.
[4] Yashchyshyn YeM. Pecularities of practical use of the terrahertz range. *ICT*. 2022;1(03):16–27.
[5] Hrychanovska TM, Protsenko IYu. Dimensional impurity effects in the crystal structure of vanadium and titanium thin films. *Visnyk Sumy State Univ Phys Mat. Mech*. 2004;10:41–50.
[6] Khalameida SV, Sydorchuk VV, Skubiszewska-Zięba J, Leboda R, Zazhigalov VO. Physical-chemical and photocatalytic properties of V-Mg oxide compositions synthesized by different methods. *Chem Phys Technol Surface*. 2013;4(1):47–54.
[7] International Centre for Diffraction Data. PDF-2 data bases for 2009. 2009. Available from: https://www.icdd.com/pdf-2/.
[8] Li F, Li Y, Wang S, Zhang J, Tang T, Liao Y, *et al.* Improved co-substituted zinc vanadate ceramics based on LTCC for enhanced polarization converters. *J Alloys Compd.* 2022;921:166089. DOI: 10.1016/j.jallcom.2022.166089.
[9] Zhang RZ, Seth S, Cumby J. Grouped representation of interatomic distances as a similarity measure for crystal structures. *Dig Discov*. 2023;2:81–90. DOI: 10.1039/D2DD00054G.
[10] Thomas JC, Natarajan AR, Van der Ven A. Comparing crystal structures with symmetry and geometry. *npj Comput Mater*. 2021;7:164. DOI: 10.1038/s41524-021-00627-0.
[11] Lin Y, Yan K, Luo Y, Liu Y, Qian X, Ji S. Efficient approximations of complete interatomic potentials for crystal property prediction. In: Proceedings of the 40th International Conference on Machine Learning. Honolulu: JMLR; 2023:21260-87.
[12] Ahmad MA, Olule LJA. Meshed stacked LTCC antenna for space application. *IEEE Access*. 2022;10:29473–81.
[13] Sadeghi M. Analysis and design of a mm-wave wideband LTCC patch antenna for 5G Applications. Calgary: University of Calgary; 2022. DOI: 10.11575/PRISM/40568.
[14] Birol H, Maeder T, Ryser P. Materials compatibility issues in LTCC technology and their effects on structural and electrical properties. In: 1st International Conference on Ceramic Interconnect and Ceramic Microsystems Technologies (CICMT); 2005:300–9.
[15] Birol H. Fabrication of low temperature co-fired ceramic (LtCC)-based sensor and micro-fluidic structures. Lausanne: EPFL; 2007.
[16] Huang YT, Huang CC, Hsu TH, Huang CL. Ultra-low temperature sintering and microwave dielectric properties of Mg-substituted $SrCoV_2O_7$ ceramics. *J Asian Ceram Soc*. 2022;10(1):188–95. DOI: 10.1080/21870764.2022.2031535.
[17] Yin C, Li C, Yang G, Fang L, Yuan Y, Shu L, Khaliq J. $NaCa_4V_5O_{17}$: A low-firing microwave dielectric ceramic with low permittivity and chemical compatibility with silver for LTCC applications. *J Eur Ceram Soc*. 2020;40(2):386–90. DOI: 10.1016/j.jeurceramsoc.2019.09.029.
[18] Unnimaya AN, Suresh EK, Ratheesh R. Crystal structure and microwave dielectric properties of new alkaline earth vanadate $A_4V_2O_9$ (A=Ba, Sr, Ca, Mg and Zn) ceramics for LTCC applications. *Mater Res Bull*. 2017;88:174–81. DOI: 10.1016/j.materresbull.2016.12.026.
[19] Zhou D, Guo D, Li WB, Pang LX, Yao X, Wang DW, Reaney IM. Novel temperature stable high-ε r microwave dielectrics in the Bi_2O_3-TiO_2-V_2O_5 system. *J Mater Chem C*. 2016;23:5357–62. DOI: 10.1039/C6TC01431C.

[20] Suresh EK, Prasad K, Arun NS, Ratheesh R. Synthesis and microwave dielectric properties of $A_{16}V_{18}O_{61}$ (A = Ba, Sr and Ca) ceramics for LTCC applications. *J Electron Mater*. 2016;45:2996–3002. DOI: 10.1007/s11664-016-4388-6.
[21] Jiang X, Li Ch, Su C, Wei Z, Fang L. Low temperature firing and microwave dielectric properties of $BaCaV_2O_7$ ceramics. *Ceram Int*. 2015;41(3B):5172–76. DOI: 10.1016/j.ceramint.2014.12.001.
[22] Wang Y, Zuo R. A novel low-temperature fired microwave dielectric ceramic $BaMg_2V_2O_8$ with ultra-low loss. *J Eur Ceram Soc*. 2016;36(1):247–51. DOI: 10.1016/j.jeurceramsoc.2015.09.011.
[23] Peng S, Li C, Tang C, Liu S, Huang S, Qiu L, Deng L. Crystal structures and microwave dielectric properties of novel $MgCu_2Nb_2O_8$ ceramics prepared by two-step sintering technique. *Materials*. 2022;15(22):8053. DOI: 10.3390/ma15228053.
[24] Barzegar-Bafrooei H, Liu B, Su W, Song KX. $Ca_3MgSi_2O_8$: Novel low-permittivity microwave dielectric ceramics for 5G application. *Mater Lett*. 2020;263:127248. DOI: 10.1016/j.matlet.2019.127248.
[25] Shivalingayya M, Raibagkar RL. Microstructure and dielectric studies of bismuth vanadate based LTCC. *Indian J Sci Res*. 2017;8(1):77–80.
[26] Bizan MS, Naseri H, Pourmohammadi P, Melouki N, Iqbal A, Denidni TA. Dual-band dielectric resonator antenna with filtering features for microwave and mm-wave applications. *Micromachines*. 2023;14(6):1236. DOI: 10.3390/mi14061236.
[27] Bataiev YM, Bataiev MM, Kornienko OA, Lavrynenko OM, Pavlenko OYu. EPR-spectral, magnetic, and ionic features of CeO2, Yb2O3, Yb2O3-CeO2 powders and ceramics based on reo oxides. *Sci Herald Uzhhorod Univ Ser Phys*. 2021; 49:9–18.
[28] Chobal I, Chobal O, Myslo Yu, Petryshynets I, Rizak V. Elastic-plastic properties of Li2B4O7 determined by nanoindentation. *Sci Herald Uzhhorod Univ Ser Phys*. 2023;53:53–63. DOI: 10.54919/physics/53.2023.53.

Кристалічна структура пірованадата $BaMnV_2O_7$

Віктор Володимирович Заводянний
Кандидат фізико-математичних наук, доцент
Херсонський державний аграрно-економічний університет
25031, просп. Університетський, 5/2, м. Кропивницький, Україна
https://orcid.org/0000-0002-8224-8215

Микола Миколайович Волошин
Кандидат технічних наук, доцент
Херсонський державний аграрно-економічний університет
25031, просп. Університетський, 5/2, м. Кропивницький, Україна
https://orcid.org/0000-0003-0467-1963

Валентина Олександрівна Зубенко
Кандидат технічних наук, доцент
Херсонський державний аграрно-економічний університет
25031, просп. Університетський, 5/2, м. Кропивницький, Україна
https://orcid.org/0000-0002-8401-755X

Руслан Васильович Телюта
Кандидат технічних наук, доцент
Центральноукраїнський національний технічний університет
25006, просп. Університетський, 8, м. Кропивницький, Україна
https://orcid.org/0000-0002-4923-1227

Сергій Олексійович Квітка
Кандидат технічних наук, доцент
Таврійський державний агротехнологічний університет імені Дмитра Моторного
69600, вул. Жуковського, 66, м. Запоріжжя, Україна
https://orcid.org/0000-0001-9234-9274

Анотація

Актуальність. Розробка матеріалів з відмінними діелектричними властивостями є важливою для сучасних телекомунікацій. Актуальність даної роботи полягає у важливості вивчення цих властивостей

в контексті розширення можливостей для високочастотних додатків у сучасних телекомунікаційних технологіях, включаючи 4G і 5G зв’язок.

Мета. Метою даного дослідження є вивчення кристалічної структури сполуки $BaMnV_2O_7$ і її діелектричних властивостей.

Методологія. Для досягнення поставленої мети використовувалися методи аналізу, експерименту, порівняння і комп’ютерного моделювання. У рамках даного дослідження було ретельно вивчено матеріал низькотемпературної спільнообпалювальної кераміки (LTCC), який відзначається високою ефективністю у якості захисту від вологи.

Результати. Була запропонована і досліджена структурна модель для сполуки $BaMnV_2O_7$. Зокрема, виявлено, що радіус Mn^{2+} (0.75 Å) майже ідентичний радіусу Zn^{2+} (0.68 Å), що підтверджує подібність кристалічних структур $BaMnV_2O_7$ та $BaZnV_2O_7$. Основні результати показали, що пірованадат має моноклінну сингонію та має просторову групу симетрії P121/c1 (14), характеризуючись такими параметрами решітки: a = 5.6221(5) Å, b = 15.271(1) Å, c = 9.7109(8) Å, β = 123.702(3)°. Фактор розбіжності склав 9.05, що свідчить про відповідність моделі експериментальним даним. Крім того, була розрахована густина сполуки, яка становить 4.2699 г/см^3.

Висновки. За допомогою експериментальних даних було підтверджено наявність міжатомних відстаней в межах 1.33-3.47 Å. Мінімальна міжатомна відстань в структурі сполуки становить 1.33 Å між атомами кисню (O5) та ванадію (V2). Максимальна міжатомна відстань складає 3.47 Å та спостерігається між атомами кисню (O1) та (O2). За характеристиками, такими як низька діелектрична проникність (εr∼8.9) та високий коефіцієнт якості (Qu×f 31362 ГГц), сполука BaMnV2O7 проявляє відмінні мікрохвильові діелектричні властивості. Практичне значення отриманих результатів полягає в можливості розвитку та вдосконалення матеріалів з високими діелектричними властивостями, таких як BaMnV2O7, для їх застосування в телекомунікаційних технологіях та сприяє розробці більш компактних та надійних компонентів для електроніки.

Ключові слова: рентгеноструктурний аналіз; діелектричні властивості; геометрія зйомки Брег-Брентано; метод Рітвельда; резонатор